HHS Public Access

Author manuscript

J Cataract Refract Surg. Author manuscript; available in PMC 2016 March 01.

Published in final edited form as:

J Cataract Refract Surg. 2015 March ; 41(3): 501–510. doi:10.1016/j.jcrs.2014.09.034.

Dynamic imaging of accommodation by swept-source anterior-segment optical coherence tomography

Alberto Neri, M.D., **Marco Ruggeri, PhD**[*], **Alessandra Protti, M.D.**, **Rosachiara Leaci, M.D.**, **Stefano A. Gandolfi, M.D.**, and **Claudio Macaluso, M.D.**

Ophthalmology, S.Bi.Bi.T. Department, University of Parma, Parma, Italy

[*]Ophthalmic Biophysics Center, Bascom Palmer Eye Institute - University of Miami Miller School of Medicine, Miami, FL

Abstract

Purpose—To study the accommodation process in normal eyes using a commercially available clinical system based on swept-source anterior-segment optical coherence tomography (SS-AS-OCT).

Setting—Ophthalmology, University of Parma, Parma, Italy.

Design—Experimental study.

Methods—The right eye of 14 healthy volunteers (18–46 years) was analyzed with SS-AS-OCT. The optical vergence of the coaxial fixation target integrated in the OCT device was adjusted during imaging to obtain monocular accommodation stimuli with different amplitudes (ASA: 0, 3, 6 and 9 Diopters). Overlapping of real and conjugate OCT images enabled imaging of all the anterior segment optical surfaces in a single frame. Intraocular distances including central corneal thickness (CCT), anterior chamber depth (ACD) and lens thickness (LT) were extracted from the OCT scans acquired at different static ASA. Dynamic analysis of the crystalline lens was also performed during accommodation and disaccommodation by sequentially acquiring OCT images of the anterior segment at a rate of 8 frames per second. LT was extracted from the temporal sequence of OCT images and plotted as a function of time.

Results—With accommodation ACD decreased significantly ($p<0.05$), LT increased ($p<0.001$) and lens central point moved slightly forward ($p<0.01$). CCT and ACW measurements did not change significantly with accommodation, which in turn confirmed that centering of the eye in the OCT images was maintained through ASA. LT at 0D was positively correlated with age (range: 3.131–4.088mm, $r=0.772$, $p<0.01$).

Conclusions—High-resolution real-time imaging and biometry of the accommodating anterior segment can be effectively performed with a commercial SS-AS-OCT clinical device.

Corresponding author: Alberto Neri, Ophthalmology, University of Parma, Via Gramsci 14, 43126 Parma, PR, Italy, Tel: +39-0521-703371, Fax: +39-0521-992137, neri.mail2@gmail.com.

FINANCIAL DISCLOSURES: no author has financial or proprietary interest in any material or method mentioned.

Keywords

accommodation; swept-source OCT; anterior segment OCT; lens imaging; dynamic OCT imaging

INTRODUCTION

The accommodation mechanism adjusts the dioptric power of the eye in order to obtain clear retinal images while looking at objects at different distances.[1] The loss of near vision with age due to presbyopia or following cataract surgery is one of the most common complaints reported by patients to general ophthalmologists. In consideration of the widespread impact that a medical procedure designed to restore accommodation may have on the ageing population a great amount of interest has been invested in the field of presbyopia research. Despite the basic of the model of accommodation was proposed by Helmoltz in 1855,[1] the mechanisms of accommodation and presbyopia are still not completely understood.[2] Providing cross-sectional imaging technology for detailed evaluation of the eye *in vivo* and in real-time is technically challenging but could help us better understand the mechanisms of accommodation and presbyopia and in the long term set the foundations for new procedures and implants aimed to restore dynamic accommodation. Magnetic resonance imaging (MRI),[3–5] ultrasound biomicroscopy (UBM),[6–8] and Scheimpflug camera (SC) based optical systems[5, 9–11] have been used to study the anatomical changes occurring in the eye during accommodation. In the past few years, optical coherence tomography (OCT) has been increasingly used to study accommodation *in vivo* and in real-time[12–30] since it has several advantages over the other ophthalmic imaging technologies. OCT enables non-contact high-resolution imaging and biometry of ocular structures with high-speed, is capable of 3D imaging and can integrate coaxial accommodative targets to stimulate accommodation in physiological conditions. Recently, a new implementation of OCT known as swept-source anterior-segment OCT (SS-AS-OCT) became available for clinical use.[31–33] Swept-source OCT is a time-encoded Fourier-Domain (FD) OCT technology based on a wavelength tunable laser source, which is characterized by very high imaging rate.[34] Biometric measurements of the anterior segment structures performed by SS-AS-OCT showed high reliability and repeatability.[31–33]

In the present study we demonstrated that a commercially available SS-AS-OCT (CASIA SS-1000 OCT®, Tomey Inc., Nagoya, Japan) can be used for a high-resolution static and dynamic study of the anterior segment of the eye during accommodation.

METHODS

Fourteen volunteers expressed written consent to the enrollment into the present study, which was conducted in accordance with the principles of the Declaration of Helsinki.[35] Criteria for inclusion into the study were normal visual function and normal accommodation, emmetropic or slightly hyperopic refraction (spherical equivalent between −0.5D and 1.0D, tested with the AR600 Autorefractor, Nidek Co., LTD., Hiroishi, Japan), and uncorrected distance (ETDRS tables, Precision Vision, La Salle, IL, USA) and near

(Runge Low Vision Near Card, Good-Lite Co., Elgin, IL, USA) visual acuities higher than 20/25 (LogMAR<0.1).

The right eye of each subject was imaged with a commercially available SS-AS-OCT system (CASIA SS-1000 OCT®, Tomey Inc., Nagoya, Japan). The OCT device consists of a swept-source laser operating at a central wavelength of 1310nm, with axial resolution of 10μm (in tissue), transverse resolution of 30μm and a scan-rate of 30,000 A-scans/sec. The transverse scanning pattern is customizable within a maximal area of 16mm × 16mm while the maximum imaging depth is 9.24mm in air, which corresponds to approximately 6mm in tissue.

Simultaneous imaging of all the anterior segment structures including the cornea, the aqueous humor and the crystalline lens is necessary to perform biometry of the accommodating eye.[13, 23, 36] The imaging depth of the SS-AS-OCT was not sufficient to image the anterior segment along its entire length, which requires an axial range of about 12mm (in air). Figure 1.1 and 1.2 show OCT vertical B-scans of the anterior segment of the eye representing the anterior (Figure 1.1) and posterior (Figure 1.2) portion of the anterior segment, respectively. To overcome this limitation, OCT scans of the anterior segment were acquired by overlapping the real and the complex conjugate (mirror) images produced by the system (Figure 1.3). The depth (z-axis) of the imaging axial range was adjusted to simultaneously include the anterior and posterior surfaces of the cornea and the lens, (points A, B, D and C in Figure 1.3) into a single OCT frame. Because the image sensitivity is highest at the zero delay line, imaging was performed with the zero delay line near to the posterior iris (bottom of the OCT image at scan depth of 9.24mm in air) to enhance the visualization of the lens. The OCT scans obtained using this technique show a vertically inverted image of the posterior lens overlapped to the direct image of the anterior structures (corneal, aqueous humor and anterior portion of the lens). Although the lens internal structures are not clearly displayed, all the optical surfaces involved in the accommodation process are simultaneously displayed (Figure 1.3).

For each subject, OCT scans were acquired using this image overlapping technique at four static accommodative stimuli with different amplitude (ASA: 0D, 3D, 6D and 9D). The scanning pattern consisted of two orthogonal transverse scans aligned along the horizontal and the vertical meridians, each of which was 16 mm in length and consisted of 2048 A-scans. During image acquisition, subjects were asked to fixate the coaxial accommodative target internal to the OCT device (hot-air balloon). The accommodation stimulus amplitude was set using the automated system of swinging lenses internal to the OCT device, placed in front of the fixation target. The scans were excluded from further analysis if the subject indicated that was unable to accommodate to a specific ASA. The OCT system also integrates an active eye-tracker that automatically centered the axes of the horizontal (x-) and vertical (y-) transverse scans to the corneal reflex.

The dynamic accommodative response to an accommodation stimulus stepping from 0D to the maximal ASA was also imaged with OCT in the same eye for each subject (Video 1). A second OCT video of dynamic accommodation was recorded for each subject during relaxation for an accommodation stimulus stepping from the maximal ASA to 0D (Video 2).

During the experiments, the participants were instructed to fixate the coaxial target of the OCT while the optical vergence of the accommodation target was changed from 0D to the maximal ASA (Video 1), or in the opposite direction (Video 2), simultaneously with the start of the image acquisition. Centering of the eye was automatically maintained during imaging by the active eye-tracker of the OCT system. Each video consisted of 38 OCT horizontal and vertical scans acquired at an imaging rate of 8 frame per second for a total duration of 4.625 sec. For dynamic imaging, the scanning pattern was adjusted so that the transversal horizontal and the vertical scans were 12.0mm in length and consisted of 512 A-scans (Figure 2 A–B, Video 1 and Video 2).

The following intraocular distances were extracted from the OCT images acquired along the vertical meridian using the linear measurements tool provided with the software of the SS-AS-OCT: central corneal thickness (CCT), anterior chamber width (ACW: distance between angular recesses), anterior chamber depth (ACD: distance from the endothelium to the anterior surface of the crystalline lens along the fixation axis) and lens thickness (LT: distance between the anterior and the posterior lens surface along the fixation axis). Lens central point (LCP: CCT+ACD+1/2LT) and anterior segment length (ASL: CCT+ACD+LT) were calculated from the measurements. LT was measured and plotted as a function of time for the dynamic responses recorded during accommodation and disaccommodation.

Intraocular optical distances were directly measured on the OCT images (Figure 1). Geometrical lengths were obtained by scaling the measured optical lengths by the group refractive index of each ocular component: 1.389 and 1.343 for cornea and aqueous humor, respectively (User Manual of CASIA SS-1000 OCT®), and 1.421 as average refractive index for the crystalline lens.[37] ACW measurements were obtained from the same images after performing automated correction with the OCT software that accounts for the difference between optical and geometrical lengths and for the image warping due to refraction of the OCT scanning beam at the different ocular surfaces.[38]

A single experienced operator acquired all the OCT scans and performed the biometric measurements using the OCT software. The same operator repeated the measurements at one-week distance in order to test the intersession repeatability of the semi-manual measuring procedure. Biometric measurements were compared among the ASA using the Wilcoxon test for pair-comparisons and the Friedman's ANOVA for multiple comparisons. Intersession repeatability was analyzed using the Intra-class Correlation Coefficient and the Coefficient of Repeatability (CR=1.96*standard deviation of the differences between repeated measurements). The statistical analysis was performed with the software Excel 2008 (Microsoft Co.) and StatPlus:mac 2009 (AnalystSoft Inc.).

RESULTS

Six male and eight female volunteers with mean age±SD=25.42±8.21 years (range=18–46 years) were included into the study. The uncorrected visual acuity (mean logMAR±SD) was −0.043±0.05 and −0.022±0.07 for distance and near vision, respectively, and refraction (mean equivalent sphere±SD) was −0.25±0.25D. Twelve out of fourteen younger participants (age < 30 years) completed all the experiments (ASA at 0 – 3 – 6 – 9D) while

the two older participants with age of 42 and 46 years only completed the experiments with ASA 0D – 6D and 0D – 3D, respectively.

The mean intraocular geometrical distances obtained at each ASA and their variations with accommodation are shown in Table 1 and 2, and in Figure 3. At ASA 0D the following biometric measurements were obtained (mean±SD): CCT=0.550±0.032mm, ACD=3.031±0.206mm, ACW=11.975±0.419mm, LT=3.5440.254mm, LCP=5.435±0.186mm, and ASL=7.207±0.221mm. LT at ASA 0D showed a positive correlation with age (r=0.772, p<0,01). CCT and ACW measurements did not show any change with accommodation (p=0.064 and 0.78, respectively). The ACD decreased (mean variation per-diopter±SD=0.027±0.012mm, p<0.05) while the LT increased (mean variation per-diopter±SD=0.036±0.013mm, p<0.001) significantly for increasing ASA. The variation of ACD and LT were proportional to the stimulus magnitude in diopters (p<0.0001) with r= −0.804 and r=0.724 for ACD and LT, respectively. The ASL (CCT+ACD+LT) did not show significant changes with accommodation (mean variation per-diopter ±SD=0.009±0.0085mm, p=0.052), while the LCP moved slightly forward for increasing ASA (mean variation per-diopter±SD=−0.009±0.0080mm, p<0.01) (Table 2, Figure 3). Figure 4 shows the results of the analysis of lens thickness dynamics during accommodation (left-hand side) and during the relaxation (right-hand side), reported for participants 9 (18 y/o), 5 (25 y/o), 11 (27 y/o) and 14 (46 y/o). The intersession repeatability of the biometric measurements was excellent, with Intra-class Correlation Coefficients 0.942, 0.998, and 0.991, and Coefficients of Repeatability 0.026, 0.035, and 0.057mm for CCT, ACD and LT measurements, respectively.

DISCUSSION

It is known that the accommodation process occurs through changes in shape and thickness of the crystalline lens.[1, 2] These changes during near vision, according to Helmholtz's theory and other experimental findings,[1, 2] are induced by the contraction of the ciliary muscle that causes the release of the zonular fibers anchored to the equator of the crystalline lens. As a consequence, the thickness and the curvature of the lens increase causing an increase in refractive power of the eye. Being a muscle-induced activity, accommodation is a highly fluctuant and a dynamic process.[2]

Time-domain OCT (TD-OCT) has been used to perform biometry of the anterior segment at different static degrees of accommodation and ages[14, 20, 24, 26, 28–30] with low image resolution and limited axial range. The imaging speed of TD-OCT systems is relatively slow, which prevents dynamic imaging of accommodation with this technology.

The more recent Fourier-domain OCT technology, including Spectral-domain (SD) and swept-source (SS) OCT implementations, provides high axial resolution and the high imaging rate that is required for dynamic analysis of accommodation.[12, 13, 15–17, 23, 25, 36] The main limitations of commercial FD-OCT implementations are the relatively short axial range and the sensitivity decay with depth, which prevent simultaneous visualization of all the optical components of the anterior segment in a single frame. In the past few years, an

effort has been made to increase the imaging depth range and improve the sensitivity performance of FD-OCT systems.

Imaging of the entire anterior segment along its whole depth has been obtained with experimental SD-OCT devices employing complex phase-splitting techniques for conjugate removal,[39, 40] dual-channel dual-focus SD-OCT devices[25] and by merging OCT images consecutively acquired at different depths with SD implementations using switchable reference arms.[12, 15, 36] SS-OCT with long imaging range (~ 12mm in air) has been demonstrated using high-speed reflective Fabry-Perot tunable lasers (RFPTL) with long coherence length that enables entire anterior segment imaging without the need of complex conjugate removal or switching of the reference arm.[13, 23] A new MEMS-VCSEL light source was recently developed for SS-OCT imaging at ultrahigh imaging rates (60kHz–1MHz) and with very long coherence depth (~50mm) that enables imaging of the entire eye.[41] This advanced SS-OCT implementation could offer significant advantages over the previous systems used for dynamic imaging of the anterior segment but, to the best of our knowledge, a study of dynamic accommodation using this technology has not been reported.

In the present work an unmodified commercially available SS-AS-OCT clinical device was used for imaging and performing biometry of dynamic accommodation. Despite the insufficient scan depth of the device (9.24mm in air), simultaneous imaging of all the anterior segment surfaces was achieved by acquiring OCT scans with overlapping real and the conjugate images (Figure 1). No modifications of the hardware and software of the SS-AS-OCT were necessary to image and obtain intraocular distances of the anterior segment at different accommodative states. The main limitation of this approach is that the internal structures of the crystalline lens cannot be clearly distinguished and measured because of the overlapping of the real and the conjugate images of the lens. Another limitation is that the posterior part of the crystalline lens is shown vertically inverted and displaced along the z-axis and therefore the images cannot be corrected for distortion due to refraction of the OCT beam at the different ocular boundaries using the software provided with the clinical system. Hence, corrected non-axial measurements such as curvature measurements or lateral distances could not be performed posteriorly to the anterior surface of the lens. A relatively simple solution to correct for full image distortion could be developing a custom-made software for boundary segmentation of the cornea and the lens that reposition the posterior surface of the lens with a vertical flip around the zero delay line and then performs distortion correction of the segmented boundaries using a ray tracing algorithm based on Snell's law.[38] In this case the raw images need to be exported to be able to perform post-processing segmentation and correction of the ocular boundaries.

In order to extract intraocular geometrical distances we used the refractive indices of the cornea and the aqueous provided by the quantification software of the SS-AS-OCT. No equivalent refractive index for the crystalline lens was specified by the manufacturer. To our knowledge, an equivalent refractive index of the crystalline lens has not been reported for wavelengths around 1300nm. In our study, to extract the geometrical thickness of the crystalline lens we assumed an average refractive index of 1.421, which was calculated in a previous study for OCT operating at 835nm.[37] As a consequence, all the LT measurements herein reported may be affected by a minor constant scaling factor. Moreover, it is possible

that minor changes in the average index of the lens may occur during the accommodation, due to modifications in the gradient of refractive index of the lens.[42]

The SS-AS-OCT device herein used is equipped with an active eye-tracker for automated centering of the OCT images that is expected to increase the accuracy of the measurements. Previous studies using this SS-AS-OCT device for biometric analysis of the anterior segment showed very high repeatability.[31, 32] In the present work intrasession repeatability of the measurements was not assessed. However, manual measurements carried out with the software of the SS-AS-OCT device showed good intersession repeatability at one-week distance from the experiments.

The results of the present study are in accordance with the model of accommodation proposed by Helmholtz and others.[1, 2, 43] The biometric analysis showed that the lens thickness increases and the anterior chamber depth decreases with accommodation. Moreover, having performed biometry at different steps of accommodation (ASA), we found that the variations in LT and ACD are proportional to the ASA. In the present study, the full length of the anterior segment measured from the cornea to the posterior surface of the lens (ASL) showed a slight mean increase at the accommodated states, but the variation did not result statistically significant. There is some controversy in the literature about the presence of an axial movement of the posterior surface of the lens during the accommodation. Some studies showed no movements of the posterior surface of the lens, resulting in no variations of ASL,[19] while other recent studies showed a significant increase of ASL at the accommodated states.[36, 44] This controversial topic is complicated by the fact that the average refractive index of the lens may vary with the changes of shape of the lens, biasing the measurements of ASL during the accommodation.[42]

The frame rate achieved by the OCT system (8fps) was sufficient to detect the transient response to an accommodation stimulus change and to observe the evolution of the lens shape dynamically. However, a higher scan rate would be desirable to obtain a more accurate dynamic analysis of the lens in order to detect the continuous and rapid fluctuations associated to the accommodation process.[45, 46] In the case of an eighteen year-old participant the dynamic analysis of accommodation and relaxation showed that at the end of the relaxation sequence the lens became thinner than before starting the accommodation sequence (Figure 4, case 9). We cannot document a definite explanation of this result, but most likely this behavior may be related with the eye returning with disaccommodation to an accomodative state that is more “relaxed” than before commencing the accommodation sequence, when the so called instrument-myopia was probably occurring, especially considering the young age of the subject.[47] Moreover, it has been described that the initial step destination of disaccommodative step responses tends to correspond to the cycloplegic refractive state.[48, 49]

A limitation of the present study is the absence of an objective measurement of the accommodation response. Measuring the power of the eye simultaneously with the OCT analysis, e.g. using an autorefractometer, may increase the reliability of the measurements and could give useful information about the relationship between the changes in the shape and position of the lens and the power of the eye.

In conclusion, optical coherence tomography appears the most promising technology for studying the accommodation process *in vivo*. The proposed study showed that high-resolution real-time imaging and biometry of the accommodating anterior segment can be effectively performed using a commercially available clinical instrument based on swept-source anterior-segment OCT. This OCT system is a promising tool to study the accommodation process in phakic as well as in pseudophakic eyes implanted with accommodating IOLs and could allow a better understanding of both the natural accommodative process and the existing strategies to restore accommodation.

Supplementary Material

Refer to Web version on PubMed Central for supplementary material.

Acknowledgments

Marco Ruggeri is supported by NIH 2R01EY14225, R01EY021834, 2R44EY01900, P30EY14801, Australian Gov. CRC scheme (Vision CRC), Florida Lions Eye Bank and Research to Prevent Blindness.

Alberto Neri, Alessandra Protti, Rosachiara Leaci, Stefano Gandolfi and Claudio Macaluso are supported in part by funding from University of Parma, Parma, Italy, and Grant “Programma di Ricerca Regione Universita” DGR22422007.

References

1. Helmholtz H. Ueber die Accommodation des Auges. Albrecht von Graefes Arch Ophthalmol. 1855; 2:1–74.
2. Charman WN. The eye in focus: accommodation and presbyopia. Clinical & experimental optometry: journal of the Australian Optometrical Association. 2008; 91:207–225.
3. Sheppard AL, Evans CJ, Singh KD, Wolffsohn JS, Dunne MC, Davies LN. Three-dimensional magnetic resonance imaging of the phakic crystalline lens during accommodation. Invest Ophthalmol Vis Sci. 2011; 52:3689–3697. [PubMed: 21296812]
4. Kasthurirangan S, Markwell EL, Atchison DA, Pope JM. MRI study of the changes in crystalline lens shape with accommodation and aging in humans. J Vis. 2011; 11:1–16.
5. Hermans EA, Pouwels PJ, Dubbelman M, Kuijer JP, van der Heijde RG, Heethaar RM. Constant volume of the human lens and decrease in surface area of the capsular bag during accommodation: an MRI and Scheimpflug study. Invest Ophthalmol Vis Sci. 2009; 50:281–289. [PubMed: 18676625]
6. Choh V, Sivak JG, Irving EL, Wong W. Ultrasound biomicroscopy of the anterior segment of the enucleated chicken eye during accommodation. Ophthalmic Physiol Opt. 2002; 22:401–408. [PubMed: 12358310]
7. Balidis MO, Bunce C, Sandy CJ, Wormald RP, Miller MH. Iris configuration in accommodation in pigment dispersion syndrome. Eye (Lond). 2002; 16:694–700. [PubMed: 12439661]
8. Mora P, Sangermani C, Ghirardini S, Carta A, Ungaro N, Gandolfi S. Ultrasound biomicroscopy and iris pigment dispersion: a case–control study. Br J Ophthalmol. 2010; 94:428–432. [PubMed: 19822906]
9. Koretz JF, Cook CA, Kaufman PL. Accommodation and presbyopia in the human eye. Changes in the anterior segment and crystalline lens with focus. Invest Ophthalmol Vis Sci. 1997; 38:569–578. [PubMed: 9071209]
10. Koretz JF, Cook CA, Kaufman PL. Aging of the human lens: changes in lens shape upon accommodation and with accommodative loss. J Opt Soc Am A Opt Image Sci Vis. 2002; 19:144–151. [PubMed: 11778717]
11. Hermans E, Dubbelman M, van der Heijde R, Heethaar R. The shape of the human lens nucleus with accommodation. J Vis. 2007; 7(16):11–10.

12. Shao Y, Tao A, Jiang H, Shen M, Zhong J, Lu F, Wang J. Simultaneous real-time imaging of the ocular anterior segment including the ciliary muscle during accommodation. Biomed Opt Express. 2013; 4:466–480. [PubMed: 23504546]
13. Satoh N, Shimizu K, Goto A, Igarashi A, Kamiya K, Ohbayashi K, Furukawa H. Accommodative changes in human eye observed by Kitasato anterior segment optical coherence tomography. Japanese journal of ophthalmology. 2013; 57:113–119. [PubMed: 23179763]
14. Richdale K, Bailey MD, Sinnott LT, Kao CY, Zadnik K, Bullimore MA. The effect of phenylephrine on the ciliary muscle and accommodation. Optom Vis Sci. 2012; 89:e1507–1511.
15. Du C, Shen M, Li M, Zhu D, Wang MR, Wang J. Anterior Segment Biometry during Accommodation Imaged with Ultralong Scan Depth Optical Coherence Tomography. Ophthalmology. 2012; 119:2479–2485. [PubMed: 22902211]
16. Malyugin BE, Shpak AA, Pokrovskiy DF. Accommodative changes in anterior chamber depth in patients with high myopia. J Cataract Refract Surg. 2012; 38:1403–1407. [PubMed: 22814046]
17. Lewis HA, Kao CY, Sinnott LT, Bailey MD. Changes in ciliary muscle thickness during accommodation in children. Optom Vis Sci. 2012; 89:727–737. [PubMed: 22504329]
18. Lossing LA, Sinnott LT, Kao CY, Richdale K, Bailey MD. Measuring changes in ciliary muscle thickness with accommodation in young adults. Optom Vis Sci. 2012; 89:719–726. [PubMed: 22504328]
19. Yuan Y, Chen F, Shen M, Lu F, Wang J. Repeated measurements of the anterior segment during accommodation using long scan depth optical coherence tomography. Eye Contact Lens. 2012; 38:102–108. [PubMed: 22223160]
20. Sheppard AL, Davies LN. The effect of ageing on in vivo human ciliary muscle morphology and contractility. Invest Ophthalmol Vis Sci. 2011; 52:1809–1816. [PubMed: 21071738]
21. Shen M, Wang MR, Yuan Y, Chen F, Karp CL, Yoo SH, Wang J. SD-OCT with prolonged scan depth for imaging the anterior segment of the eye. Ophthalmic Surg Lasers Imaging. 2010; 41(Suppl):S65–69. [PubMed: 21117604]
22. Yan PS, Lin HT, Wang QL, Zhang ZP. Anterior segment variations with age and accommodation demonstrated by slit-lamp-adapted optical coherence tomography. Ophthalmology. 2010; 117:2301–2307. [PubMed: 20591484]
23. Furukawa H, Hiro-Oka H, Satoh N, Yoshimura R, Choi D, Nakanishi M, Igarashi A, Ishikawa H, Ohbayashi K, Shimizu K. Full-range imaging of eye accommodation by high-speed long-depth range optical frequency domain imaging. Biomed Opt Express. 2010; 1:1491–1501. [PubMed: 21258564]
24. Sheppard AL, Davies LN. In vivo analysis of ciliary muscle morphologic changes with accommodation and axial ametropia. Invest Ophthalmol Vis Sci. 2010; 51:6882–6889. [PubMed: 20671285]
25. Zhou C, Wang J, Jiao S. Dual channel dual focus optical coherence tomography for imaging accommodation of the eye. Opt Express. 2009; 17:8947–8955. [PubMed: 19466144]
26. Konradsen TR, Koivula A, Kugelberg M, Zetterstrom C. Accommodation measured with optical coherence tomography in patients with Marfan's syndrome. Ophthalmology. 2009; 116:1343–1348. [PubMed: 19427698]
27. Schultz KE, Sinnott LT, Mutti DO, Bailey MD. Accommodative fluctuations, lens tension, and ciliary body thickness in children. Optom Vis Sci. 2009; 86:677–684. [PubMed: 19417700]
28. Richdale K, Bullimore MA, Zadnik K. Lens thickness with age and accommodation by optical coherence tomography. Ophthalmic Physiol Opt. 2008; 28:441–447. [PubMed: 18761481]
29. Baikoff G, Lutun E, Ferraz C, Wei J. Static and dynamic analysis of the anterior segment with optical coherence tomography. J Cataract Refract Surg. 2004; 30:1843–1850. [PubMed: 15342045]
30. Baikoff G, Lutun E, Wei J, Ferraz C. Anterior chamber optical coherence tomography study of human natural accommodation in a 19-year-old albino. J Cataract Refract Surg. 2004; 30:696–701. [PubMed: 15050270]
31. Neri A, Malori M, Scaroni P, Leaci R, Delfini E, Macaluso C. Corneal thickness mapping by 3D swept-source anterior segment optical coherence tomography. Acta Ophthalmol. 2012; 90:e452–e457. [PubMed: 22682316]

32. Fukuda S, Kawana K, Yasuno Y, Oshika T. Repeatability and reproducibility of anterior chamber volume measurements using 3-dimensional corneal and anterior segment optical coherence tomography. J Cataract Refract Surg. 2011; 37:461–468. [PubMed: 21333870]
33. Liu S, Yu M, Ye C, Lam DS, Leung CK. Anterior chamber angle imaging with swept-source optical coherence tomography: an investigation on variability of angle measurement. Invest Ophthalmol Vis Sci. 2011; 52:8598–8603. [PubMed: 21948547]
34. Yun S, Tearney G, de Boer J, Iftimia N, Bouma B. High-speed optical frequency-domain imaging. Opt Express. 2003; 11:2953–2963. [PubMed: 19471415]
35. The World Medical Association (WMA). The WMA declaration of Helsinki 1960 with recommendations on biomedical research on human subjects (modified in 1975, 1980 and 1989). Chirurgia. 1998; 93:138–140. [PubMed: 9696606]
36. Ruggeri M, Uhlhorn SR, De Freitas C, Ho A, Manns F, Parel JM. Imaging and full-length biometry of the eye during accommodation using spectral domain OCT with an optical switch. Biomed Opt Express. 2012; 3:1506–1520. [PubMed: 22808424]
37. de Freitas C, Ruggeri M, Manns F, Ho A, Parel JM. In vivo measurement of the average refractive index of the human crystalline lens using optical coherence tomography. Opt Lett. 2013; 38:85–87. [PubMed: 23454923]
38. Westphal V, Rollins A, Radhakrishnan S, Izatt J. Correction of geometric and refractive image distortions in optical coherence tomography applying Fermat's principle. Opt Express. 2002; 10:397–404. [PubMed: 19436373]
39. Jungwirth J, Baumann B, Pircher M, Gotzinger E, Hitzenberger CK. Extended in vivo anterior eye-segment imaging with full-range complex spectral domain optical coherence tomography. J Biomed Opt. 2009; 14:050501. [PubMed: 19895097]
40. Grulkowski I, Gora M, Szkulmowski M, Gorczynska I, Szlag D, Marcos S, Kowalczyk A, Wojtkowski M. Anterior segment imaging with Spectral OCT system using a high-speed CMOS camera. Opt Express. 2009; 17:4842–4858. [PubMed: 19293916]
41. Grulkowski I, Liu JJ, Potsaid B, Jayaraman V, Lu CD, Jiang J, Cable AE, Duker JS, Fujimoto JG. Retinal, anterior segment and full eye imaging using ultrahigh speed swept source OCT with vertical-cavity surface emitting lasers. Biomed Opt Express. 2012; 3:2733–2751. [PubMed: 23162712]
42. Dubbelman M, Van der Heijde GL, Weeber HA, Vrensen GF. Changes in the internal structure of the human crystalline lens with age and accommodation. Vision Res. 2003; 43:2363–2375. [PubMed: 12962993]
43. Strenk SA, Strenk LM, Koretz JF. The mechanism of presbyopia. Progress in retinal and eye research. 2005; 24:379–393. [PubMed: 15708834]
44. Zhong J, Tao A, Xu Z, Jiang H, Shao Y, Zhang H, Liu C, Wang J. Whole eye axial biometry during accommodation using ultra-long scan depth optical coherence tomography. Am J Ophthalmol. 2014; 157:1064–1069. [PubMed: 24487051]
45. Heron G, Charman WN, Gray LS. Accommodation dynamics as a function of age. Ophthalmic Physiol Opt. 2002; 22:389–396. [PubMed: 12358308]
46. Heron G, Charman WN, Gray LS. Accommodation responses and ageing. Invest Ophthalmol Vis Sci. 1999; 40:2872–2883. [PubMed: 10549647]
47. Miwa T. Instrument myopia and the resting state of accommodation. Optom Vis Sci. 1992; 69:55–59. [PubMed: 1741112]
48. Bharadwaj SR, Schor CM. Dynamic control of ocular disaccommodation: first and second-order dynamics. Vision Res. 2006; 46:1019–1037. [PubMed: 16045960]
49. Bharadwaj SR, Schor CM. Initial destination of the disaccommodation step response. Vision Res. 2006; 46:1959–1972. [PubMed: 16427109]

WHAT WAS KNOWN

- An effective real-time imaging system to visualize the eye during accommodation would significantly improve the understanding of the mechanisms that govern the normal accommodation and of those that cause presbyopia, with the aim of setting the foundations for new procedures and implants designed to restore dynamic accommodation in presbyopic as well as in pseudophakic eyes.
- Fourier-domain optical coherence tomography (FD-OCT) appears the most promising technology for the study of the accommodation process *in vivo*. Major technical limitations (e.g. limited imaging depth and the decay of sensitivity with depth) have not allowed visualization of the entire anterior segment in the study of the accommodation process.

WHAT THIS PAPER ADDS

- Simultaneous OCT imaging of all the anterior segment surfaces can be done with a commercially available swept-source anterior segment OCT (SS-AS-OCT) despite the insufficient scan depth of the device by acquiring scans showing both the real and the conjugate images.
- High-resolution dynamic imaging and biometry of the accommodating anterior segment can be effectively performed using this SS-AS-OCT.
- This OCT system could become useful to study the accommodation process in both phakic and in pseudophakic eyes with accommodating IOLs.

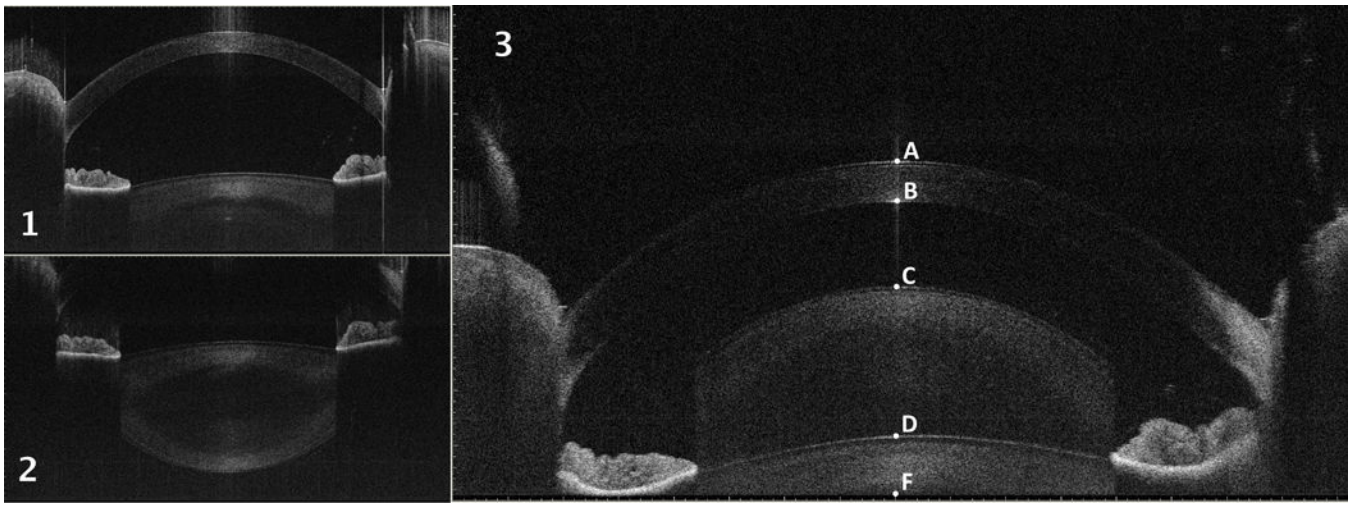

Figure 1. SS-AS-OCT scans of an eye included into the study

1. *Vertical B-scan showing the anterior part of the anterior segment*: the posterior aspect of the crystalline lens is not included into the scan.

2. *Vertical B-scan showing the posterior part of the anterior segment*: the entire crystalline lens is shown while the anterior part of the cornea is not included into the scan.

3. *Vertical B-scan showing the entire anterior segment of the eye by overlapping the real and the conjugate images*: the posterior lens is shown vertically inverted and overlapped to the anterior lens. All the optical surfaces of the anterior segment are included into the scan and the following intraocular distances can be measured: central corneal thickness (CCT): distance from point A to point B; anterior chamber depth (ACD): distance from point B to point D; lens thickness (LT): distance from point D to point F plus distance from point C to point F.

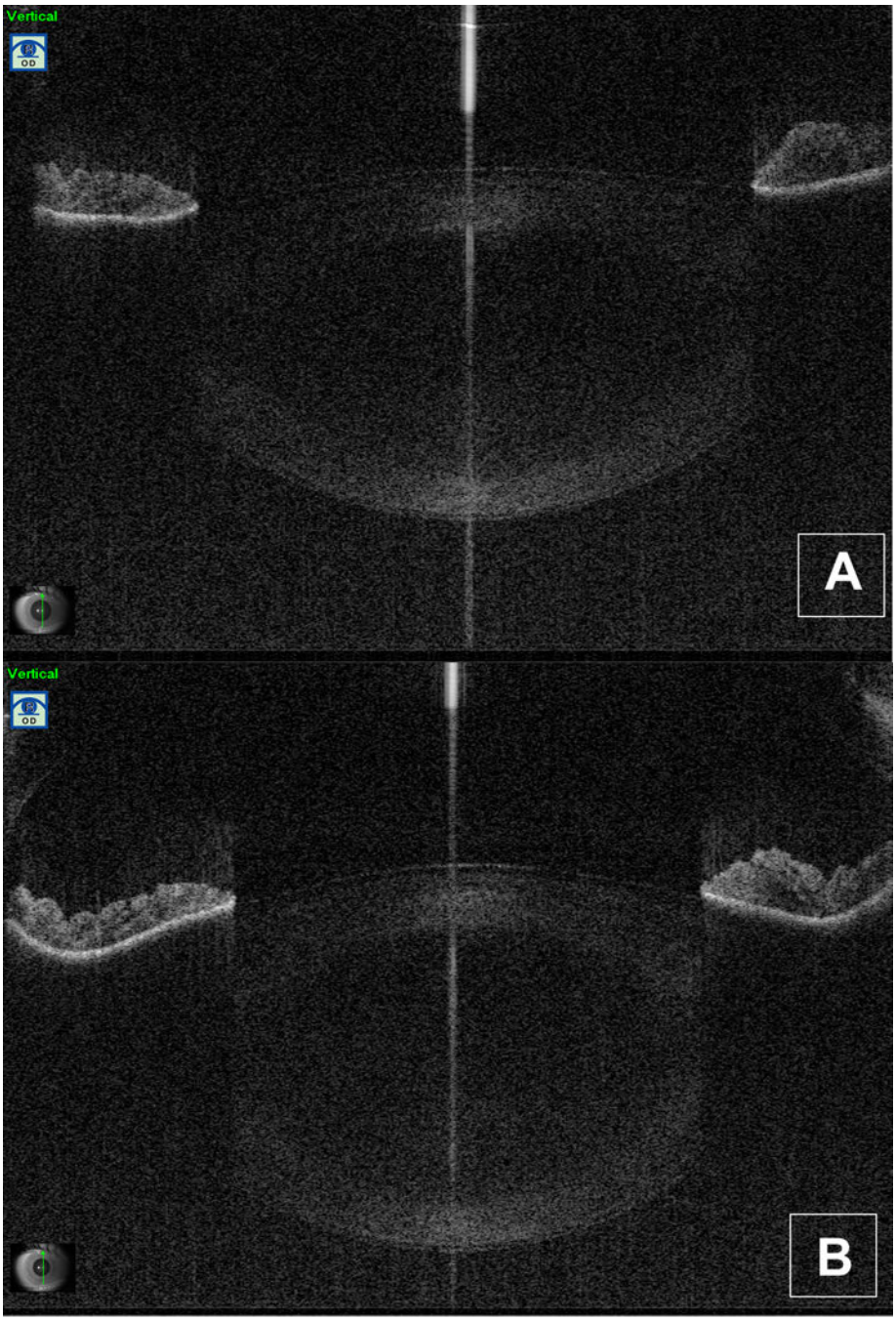

Figure 2. Example of SS-AS-OCT dynamic analysis of the crystalline lens changes in shape during the accommodation process

A. Initial frame (vertical B-scan) of video 1 (accommodation) for an eye included into the study: the lens is shown at the relaxed state (accommodation stimulus amplitude or ASA=0D).

B. Initial frame (vertical B-scan) of video 2 (relaxation from accommodation) for an eye included into the study: the eye is shown at the maximal ASA (ASA=9D).

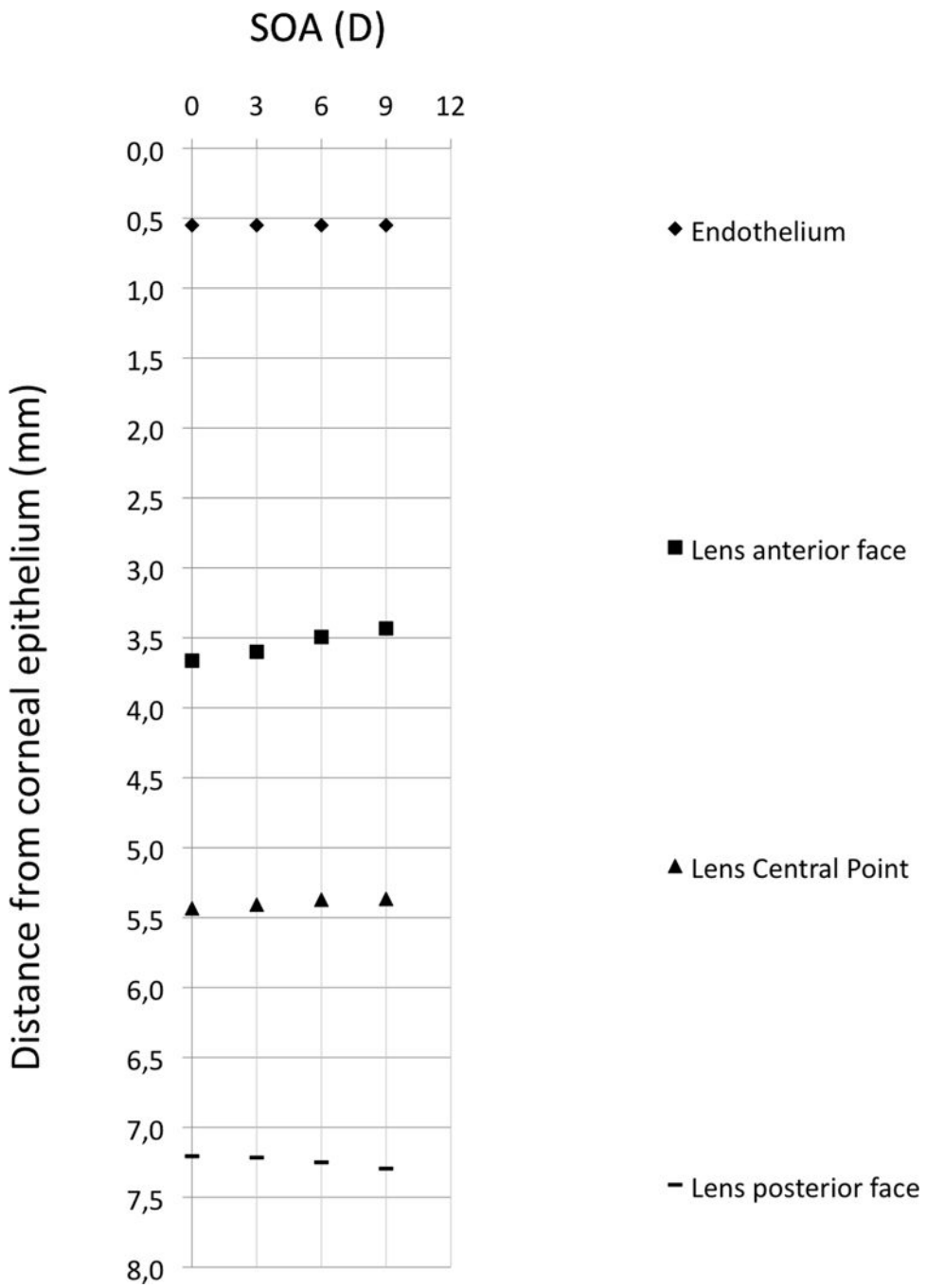

Figure 3. Graph showing the intraocular distance changes during accommodation

The graph reports the mean axial distances of the corneal endothelium, lens anterior surface face, lens central point, and lens posterior surface from the corneal epithelium for different accommodation stimulus amplitudes (ASA): 0, 3, 6, and 9D.

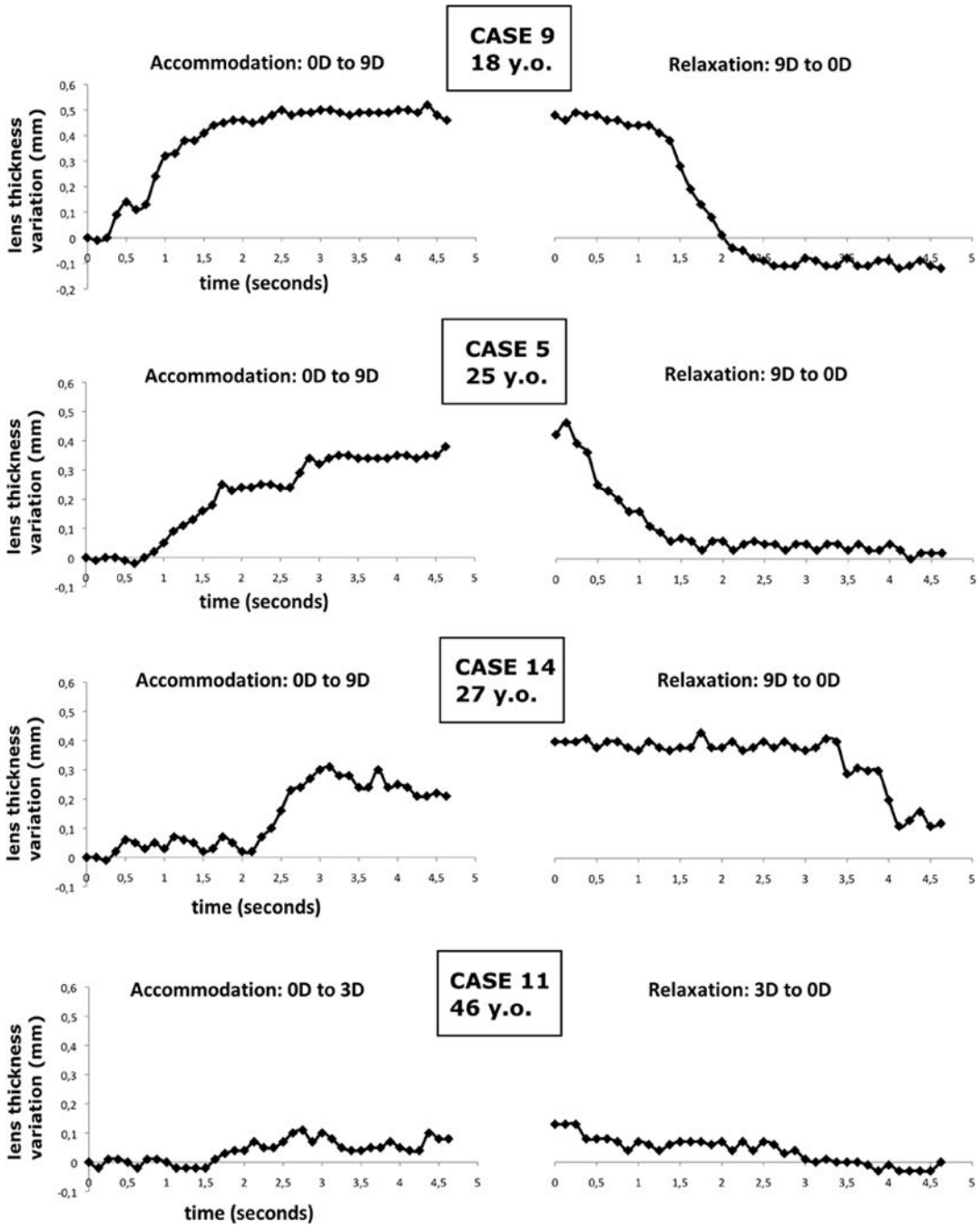

Figure 4. Dynamic biometry of accommodation for four subjects at different age

Changes in the lens thickness during accommodation are plotted in function of time. The dynamic changes of the lens thickness are reported after the stimulus onset (t=0s). The graphs on the left-hand side show the accommodation process 0D to the maximal ASA (accommodation stimulus amplitude). The graphs on the right-hand side show the relaxation process from the maximal ASA to ASA=0D.

Author Manuscript

Author Manuscript

Author Manuscript

Table 1

Intraocular distances (means±SD) at different accommodation stimulus amplitudes.

ASA	ACD (mm)	LT (mm)	LCP (mm)	ASL (mm)
0D	3.113±0.217	3.544±0.254	5.435±0.186	7.207±0.221
3D	3.050±0.216	3.616±0.251	5.408±0.181	7.216±0.214
6D	2.944±0.204	3.755±0.227	5.373±0.187	7.250±0.224
9D	2.883±0.202	3.857±0.191	5.367±0.212	7.295±0.253

ASA: accommodation stimulus amplitude; D: optical diopters; ACD: anterior chamber depth; LT: lens thickness; LCP lens central point; ASL: anterior segment length.

Table 2

mean variations (mean Δ ± SD) of the intraocular distances through different accommodation stimulus amplitudes.

ASA	ΔACD (mm)	ΔLT (mm)	ΔLCP (mm)	ΔASL (mm)
3D-0D	−0.063±0.045	0.072±0.059	−0.027±0.021	0.009±0.024
6D-0D	−0.187±0.068	0.239±0.082	−0.067±0.032	0.053±0.029
9D-0D	−0.263±0.086	0.385±0.074	−0.071±0.081	0.122±0.091
	p<0.001	p<0.001	p<0.001	p=0.052

ASA: accommodation stimulus amplitude; D: optical diopters; ΔACD: anterior chamber depth variation; ΔLT: lens thickness variation; ΔLCP: lens central point variation; ΔASL: anterior segment length variation. p-value is derived by Friedman's ANOVA for multiple comparisons.